Global Biogeochemical Cycles

Supporting Information for

The annual cycle of gross primary production, net community production and export efficiency across the North Pacific Ocean

Hilary I. Palevsky[1a], Paul D. Quay[1], Deirdre E. Lockwood[1], David P. Nicholson[2]

[1] School of Oceanography, University of Washington, Seattle, Washington, USA
[2] Marine Chemistry and Geochemistry Department, Woods Hole Oceanographic Institution, Woods Hole, Massachusetts, USA

[a] Corresponding Author:
School of Oceanography, University of Washington, Seattle, Washington 98105, USA
Email: palevsky@uw.edu

Contents of this file

Supplementary Text, including equations S1-S7
Figures S1 to S5
Tables S1 to S4

Additional supporting information (File uploaded separately)

Data Set S1: Kuroshio region winter depth profile data.
This is a CSV file containing the geochemical measurements from late winter depth profiles in the Kuroshio region (presented in Figure S3). Data columns are: Station, Cast, Niskin bottle, Latitude (°N), Longitude (°E), Depth (meters), Salinity, Temperature (°C), O_2/Ar dissolved gas ratio, $\delta^{18}O$ (per mil), $\delta^{17}O$ (per mil), and $^{17}\Delta$ (per meg).

Introduction

This supplement includes a derivation of the surface mixed layer O_2/Ar budget (equation 2 in the main text) used to estimate NCP (Supplementary Text, including equations S1-S7), a detailed breakdown of seasonal and annual GOP and NCP budget component term estimates (Tables S2-S4), visualizations of CESM model results discussed in the main text (Figures S1, S2 and S5), a visualization of the seasonal migration of the transition zone chlorophyll front (Figure S3), a sensitivity analysis for a range of potential assumptions for winter NCP used in estimating K_z (Table S1), and plots of geochemical depth profile measurements from the Kuroshio region in winter (Figure S4, full data in Data Set S1).

Supplementary Text: Derivation of surface mixed layer O_2/Ar budget to estimate NCP

The surface mixed layer O_2/Ar budget used to estimate NCP (equation (4) in the main text) and the derivation shown here, are based on previous work combining oxygen and argon budgets to estimate NCP [*Craig and Hayward*, 1987; *Howard et al.*, 2010; *Lockwood*, 2013]. We write separate mass balance equations for the effects of gas exchange, physical supply and NCP on mixed layer concentrations of dissolved oxygen and argon. Since argon is an inert gas, it is not affected by NCP. Details of the physical supply terms are given in equation (7) in the main text.

$$z_{\mathrm{ml}}\frac{\partial[\mathrm{O_2}]_{\mathrm{ml}}}{\partial t} = -\mathrm{k_{O2}}\left([\mathrm{O_2}]_{\mathrm{ml}} - [\mathrm{O_2}]_{\mathrm{eq}}\right) + z_{\mathrm{ml}}\frac{\partial \mathrm{O_2}}{\partial \mathrm{t}}_{\mathrm{phys}} + \mathrm{NCP} \quad \text{(S1)}$$

$$z_{\mathrm{ml}}\frac{\partial[\mathrm{Ar}]_{\mathrm{ml}}}{\partial t} = -\mathrm{k_{Ar}}\left([\mathrm{Ar}]_{\mathrm{ml}} - [\mathrm{Ar}]_{\mathrm{eq}}\right) + z_{\mathrm{ml}}\frac{\partial \mathrm{Ar}}{\partial \mathrm{t}}_{\mathrm{phys}} \quad \text{(S2)}$$

To write a combined budget for O_2/Ar, we multiply equation (S2) by $(O_2/Ar)_{eq}$ and subtract it from equation (S1). We make the simplifying assumption that $k_{Ar} \approx k_{O2}$, based on the similarity in solubility and molecular diffusion between the two gases.

$$z_{\mathrm{ml}}\left[\frac{\partial[\mathrm{O_2}]_{\mathrm{ml}}}{\partial t} - (\mathrm{O_2/Ar})_{\mathrm{eq}}\frac{\partial[\mathrm{Ar}]_{\mathrm{ml}}}{\partial t}\right] = -\mathrm{k_{O2}}\left([\mathrm{O_2}]_{\mathrm{ml}} - (\mathrm{O_2/Ar})_{\mathrm{eq}}[\mathrm{Ar}]_{\mathrm{ml}}\right) + z_{\mathrm{ml}}\left(\frac{\partial \mathrm{O_2}}{\partial \mathrm{t}}_{\mathrm{phys}} - (\mathrm{O_2/Ar})_{\mathrm{eq}}\frac{\partial \mathrm{Ar}}{\partial \mathrm{t}}_{\mathrm{phys}}\right) + \mathrm{NCP} \quad \text{(S3)}$$

To simplify equation (S3), we represent oxygen and argon gas supersaturation following the form:

$$\Delta \mathrm{C} = \frac{[\mathrm{C}]_{\mathrm{ml}}}{[\mathrm{C}]_{\mathrm{eq}}} - 1 \quad \text{(S4)}$$

Applying the notation of equation (S4):

$$[\mathrm{O_2}]_{\mathrm{ml}} - (\mathrm{O_2/Ar})_{\mathrm{eq}}[\mathrm{Ar}]_{\mathrm{ml}} = [\mathrm{O_2}]_{\mathrm{eq}}(\Delta \mathrm{O_2} - \Delta \mathrm{Ar}) \quad \text{(S5)}$$

The O_2-Ar supersaturation difference, (ΔO_2 - ΔAr), is commonly approximated as ΔO_2/Ar (following equation (S4) here and also defined in equation (3) in the main text). Applying this approximation and substituting into the time rate of change (left hand side) term and gas exchange (first right hand side) terms in equation (S3) following equation (S5):

$$z_{\mathrm{ml}}[\mathrm{O_2}]_{\mathrm{eq}}\frac{\partial(\Delta \mathrm{O_2/Ar})}{\partial t} = -\mathrm{k_{O2}}[\mathrm{O_2}]_{\mathrm{eq}}\Delta \mathrm{O_2/Ar} + z_{\mathrm{ml}}\left(\frac{\partial \mathrm{O_2}}{\partial \mathrm{t}}_{\mathrm{phys}} - (\mathrm{O_2/Ar})_{\mathrm{eq}}\frac{\partial \mathrm{Ar}}{\partial \mathrm{t}}_{\mathrm{phys}}\right) + \mathrm{NCP} \quad \text{(S6)}$$

Rearranging equation (S6) to solve for NCP produces the form of equation (4) presented in the main text, which is also reproduced below:

$$\mathrm{NCP} = \mathrm{k}[\mathrm{O_2}]_{\mathrm{eq}}\Delta \mathrm{O_2/Ar} + \frac{\partial(\Delta \mathrm{O_2/Ar})}{\partial t}z_{\mathrm{ml}}[\mathrm{O_2}]_{\mathrm{eq}} - z_{\mathrm{ml}}\left(\frac{\partial \mathrm{O_2}}{\partial \mathrm{t}}_{\mathrm{phys}} - (\mathrm{O_2/Ar})_{\mathrm{eq}}\frac{\partial \mathrm{Ar}}{\partial \mathrm{t}}_{\mathrm{phys}}\right) \quad \text{(S7)}$$

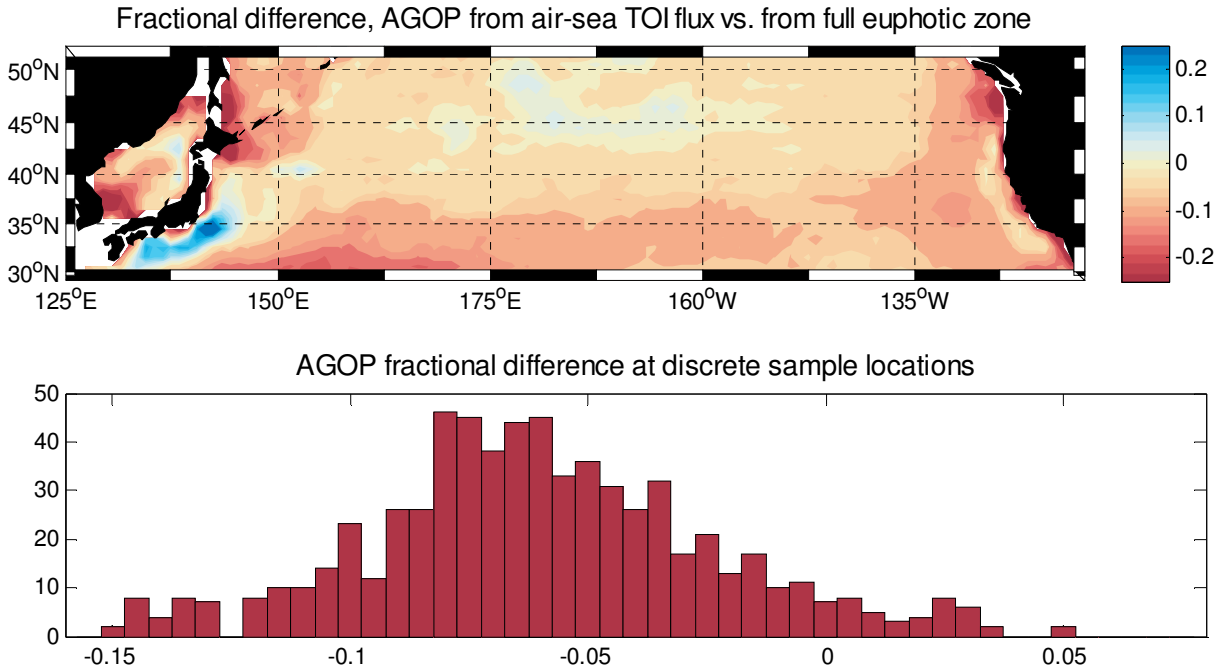

Figure S1: Comparison between North Pacific AGOP in the Community Earth System Model (CESM) as determined from the annually-integrated rate of air-sea TOI flux and from the model's reality for annual gross oxygen production (AGOP) through the full euphotic zone. The spatial map (top) shows trends in the fractional difference throughout the North Pacific, where blue (red) indicates higher (lower) estimated AGOP from annually-integrated air-sea TOI flux than the model's reality of full euphotic zone AGOP. The histogram (bottom) shows fractional offsets at the locations of all discrete sample points included in this study, with a mean offset of -0.06, indicating that AGOP from air-sea TOI flux is 6% lower than the model's reality of full euphotic zone AGOP.

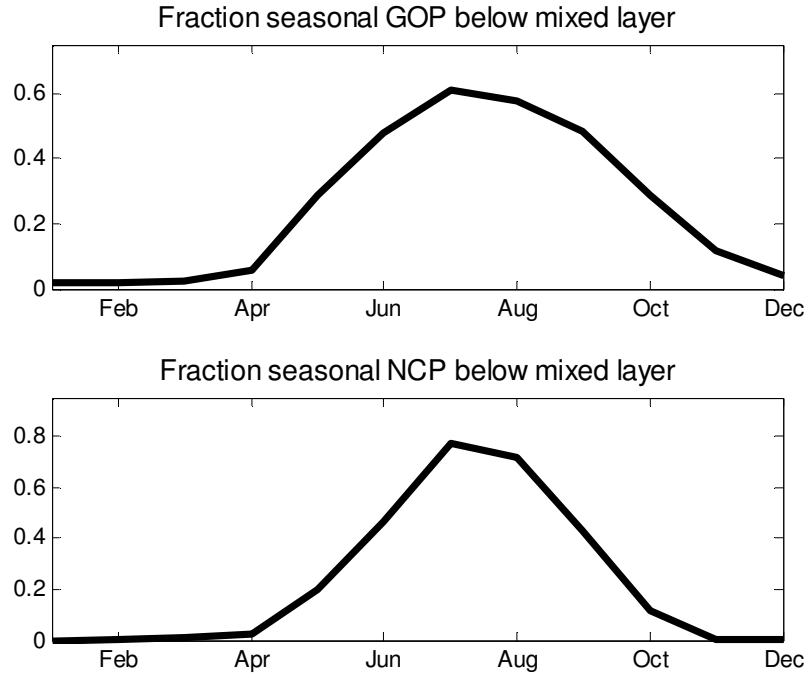

Figure S2: Fraction of monthly productivity occurring below the seasonal mixed layer in the North Pacific (35– 50 °N, 142°E – 125°W) in Community Earth System Model (CESM) output, for (top) gross oxygen production (GOP) integrated through the full euphotic zone, and (bottom) net community production (NCP), integrated to the compensation depth (where photosynthesis = respiration).

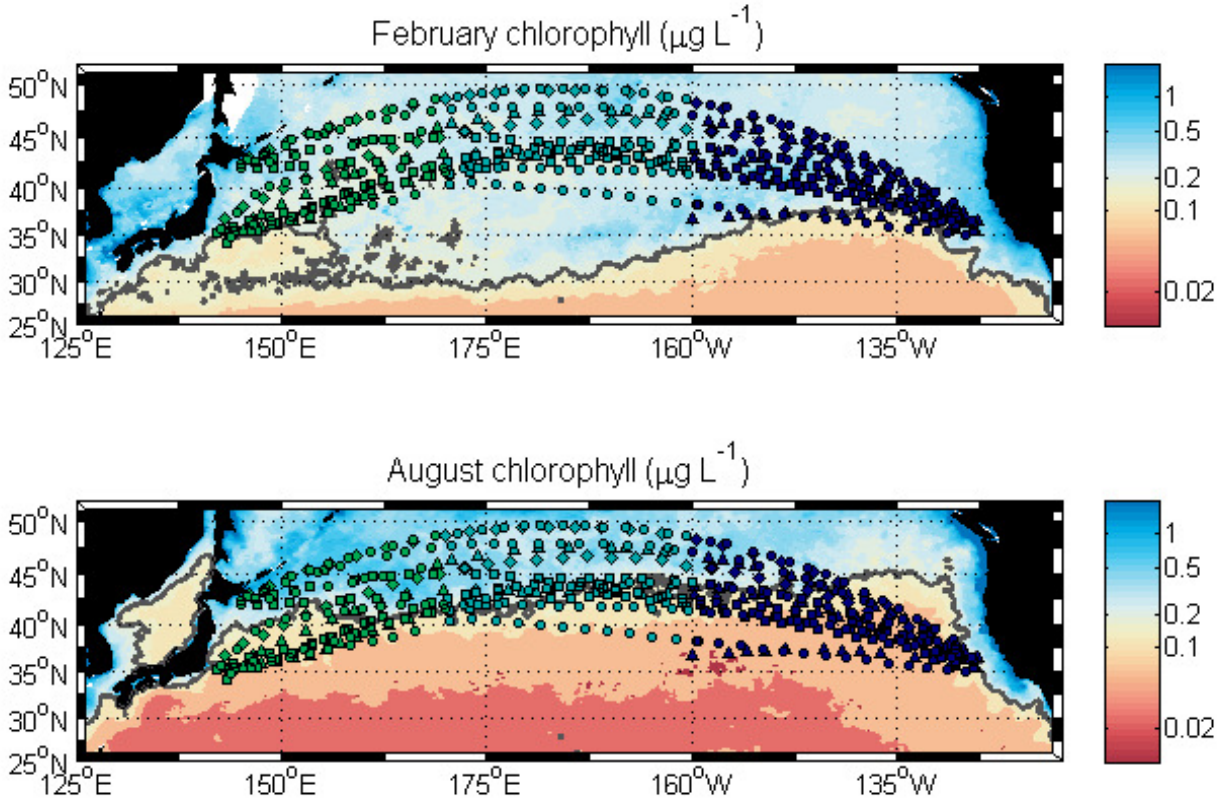

Figure S3: MODIS chlorophyll concentrations (mean of 2008-2012 data) for February (top) and August (bottom), which are the months of the southernmost and northernmost locations respectively of the transition zone chlorophyll front (TZCF; defined by the 0.2 μg L^{-1} chlorophyll isopleth, dark gray line). Locations of mixed layer discrete samples from container ship transects (as in Figure 1) are shown for reference. Regions discussed in the main paper are the Kuroshio (green), the Western region (light blue), and the Eastern region (dark blue). The annual cycle is divided by season: spring (Mar. – May, triangles), summer (June – Aug., diamonds), fall (Sept. – Nov., squares), and winter (Dec. – Feb., circles).

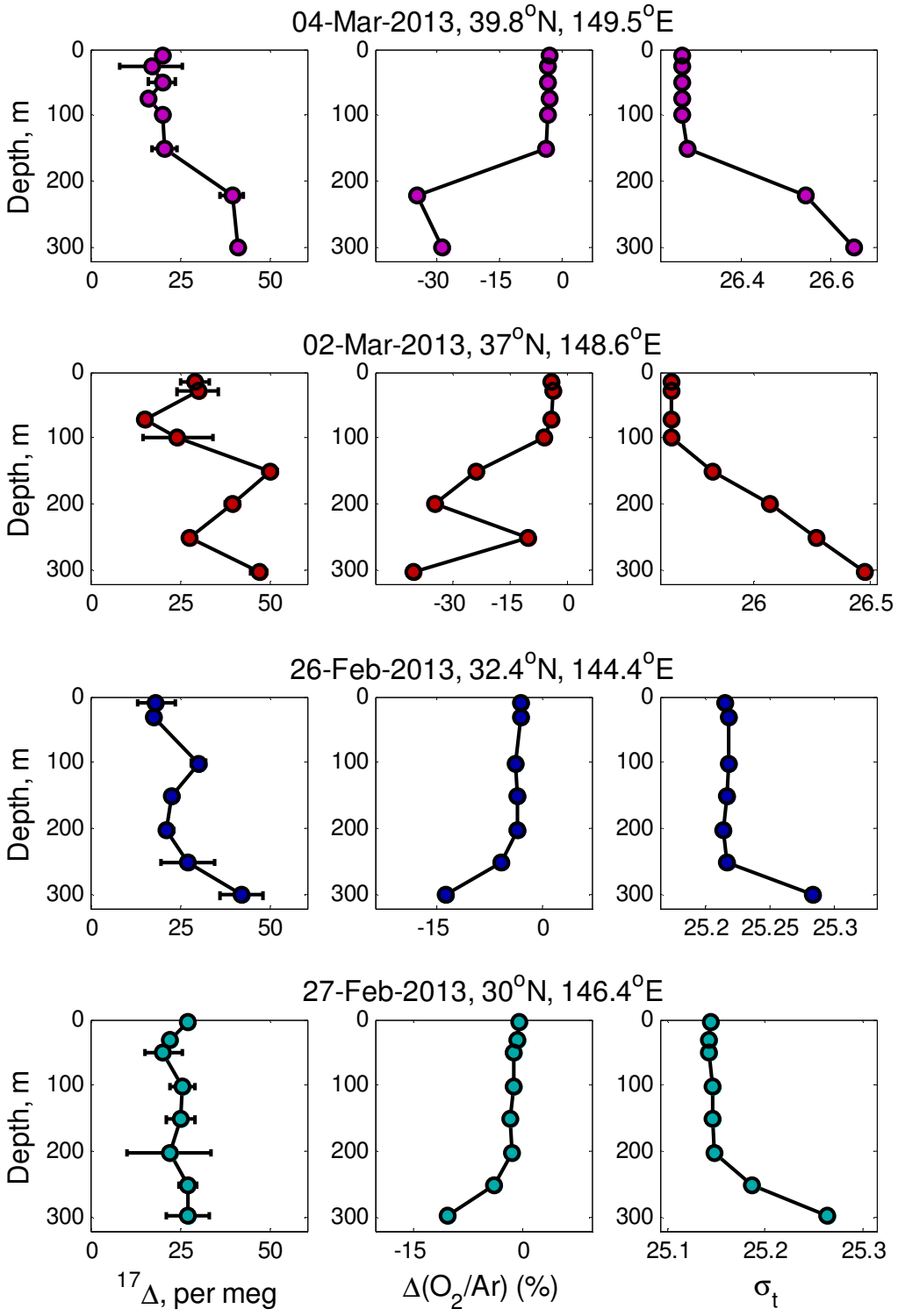

Figure S4: Depth profiles for TOI ($^{17}\Delta$), $\Delta O_2/Ar$, and density (σ_t) for four locations in the Kuroshio region in late winter. Error bars show the full range between measurements from duplicate samples. Profile locations are shown in the map in Figure 1 and constraints on wintertime GOP and NCP from these data are shown in Figure 5, both with colors corresponding to those shown here.

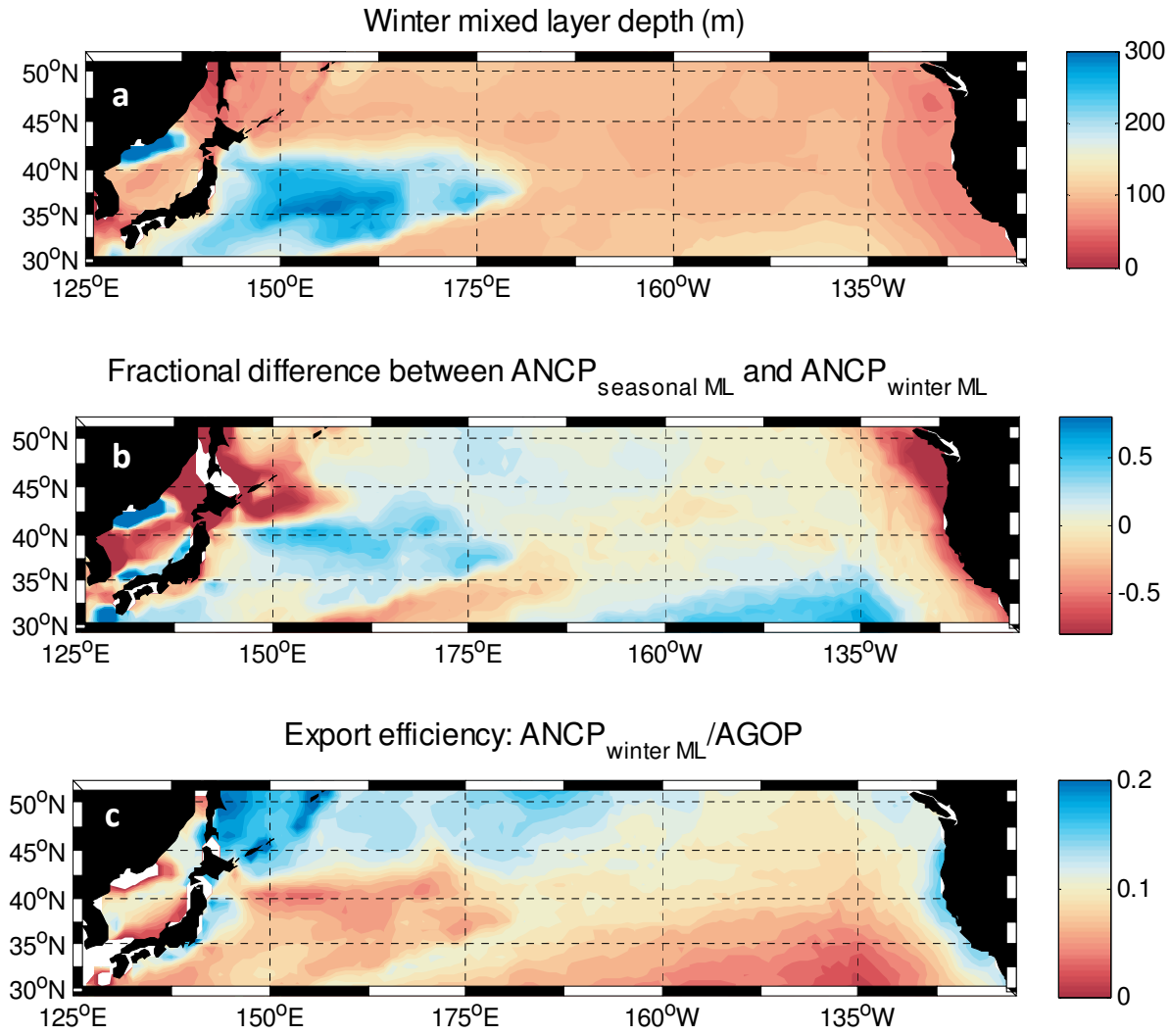

Figure S5: Community Earth System Model (CESM) output in the North Pacific for a) the maximum annual (winter) mixed layer depth, b) the fractional difference between annual net community production (ANCP) to the base of the seasonally-varying mixed layer and to the winter mixed layer depth, such that positive values (blue) represent lower ANCP at the winter mixed layer depth due to remineralization of organic matter between the base of the seasonal mixed layer and the winter mixing depth and negative values (red) represent greater ANCP at the winter mixed layer depth due to a net autotrophic sub-mixed layer, and c) annual export efficiency, defined as the fraction of annual gross oxygen production (AGOP) through the full euphotic zone that contributes to ANCP to the winter mixed layer depth.

Table S1: Influence of varying assumptions for winter NCP on K_z and on the mixed layer NCP budget [a]

	Winter NCP = -10	Winter NCP = -5	Winter NCP = 0 [b]	Winter NCP = 5	Winter NCP = 10
Kuroshio					
Winter K_z	3.1×10^{-4}	4.1×10^{-4}	5.1×10^{-4}	6.1×10^{-4}	7.1×10^{-4}
Spring (MAM)	22.7 ± 4.5	25.0 ± 5.4	27.2 ± 6.5	29.5 ± 7.4	31.7 ± 8.6
Summer (JJA)	16.2 ± 2.5	16.2 ± 2.4	16.2 ± 2.4	16.1 ± 2.5	16.1 ± 2.4
Fall (SON)	19.4 ± 11.5	19.7 ± 11.5	20.0 ± 11.6	20.3 ± 11.5	20.6 ± 11.5
Annual	4.4 ± 1.9	5.1 ± 2.1	5.8 ± 2.2	6.5 ± 2.6	7.2 ± 2.9
West					
Winter K_z	[c]	[c]	3.6×10^{-5}	1.4×10^{-4}	2.3×10^{-4}
Spring (MAM)	--	--	20.9 ± 4.4	24.0 ± 4.7	27.0 ± 5.2
Summer (JJA)	--	--	14.9 ± 2.6	15.0 ± 2.6	15.1 ± 2.6
Fall (SON)	--	--	15.2 ± 2.8	15.2 ± 2.9	15.2 ± 2.8
Annual	--	--	4.7 ± 1.0	5.4 ± 1.1	6.1 ± 1.2
East					
Winter K_z	[b]	[b]	[b] 2.0×10^{-5}	6.5×10^{-5}	2.2×10^{-4}
Spring (MAM)	--	--	12.8 ± 2.3	14.2 ± 2.5	19.0 ± 4.1
Summer (JJA)	--	--	5.3 ± 0.9	4.8 ± 1.0	3.1 ± 1.6
Fall (SON)	--	--	18.7 ± 3.0	18.6 ± 3.1	18.2 ± 3.1
Annual	--	--	3.7 ± 0.6	3.9 ± 0.6	4.6 ± 0.7

[a] Winter vertical diffusivity at the base of the mixed layer (K_z, units of $m^2\ s^{-1}$) is determined from a range of assumptions for winter net heterotrophy or autotrophy rates. Applying this value for K_z, resulting seasonal mixed layer NCP for spring through fall (mmol $O_2\ m^{-2}\ d^{-1}$) and annual NCP integrated to the base of the mixed layer in each season (mol $O_2\ m^{-2}\ yr^{-1}$) are also determined. The majority of the difference in the annual NCP estimated from the mixed layer budget results from changes in winter NCP, since an increase of 5 mmol $O_2\ m^{-2}\ d^{-1}$ in winter NCP adds 0.5 mol $O_2\ m^{-2}\ yr^{-1}$ to the annual mixed layer NCP. ANCP integrated to the winter ventilation depth is not affected by changes in K_z. Values based on the assumption of winter NCP = 0 are used throughout the main paper.

[b] Eliminating the influence of vertical diffusion (setting $K_z = 0$) only reduces wintertime NCP in the Eastern region to 2.9 mmol $O_2\ m^{-2}\ d^{-1}$. For the main paper, we assume K_z in the summer and fall at a background value of $1.0 \times 10^{-5}\ m^2\ s^{-1}$ and double this value for winter and spring K_z, yielding winter NCP of 3.5 mmol $O_2\ m^{-2}\ d^{-1}$.

[c] Eliminating the influence of vertical diffusion (setting $K_z = 0$) only reduces wintertime NCP in the Western region to -1.8 mmol $O_2\ m^{-2}\ d^{-1}$.

Table S2: Seasonal means for each region for all terms in the gross oxygen production (GOP) mixed layer budget[a]

Kuroshio							
	Air-sea TOI flux	Non-steady state	Physical supply				Gross oxygen production (GOP)
			Vertical supply	Upwelling	Horizontal convergence	Sum	
Spring (MAM)	253 ± 55 (98)	7.7 ± 3.9	25.1 ± 12.5	-1.9 ± 1.0	-2.2 ± 1.1	21.0 ± 12.6	238 ± 57 (85)
Summer (JJA)	147 ± 24 (48)	-0.8 ± 0.4	43.7 ± 21.9	-0.6 ± 0.3	-7.4 ± 3.7	35.7 ± 22.2	108 ± 33 (33)
Fall (SON)	202 ± 113 (131)	-6.6 ± 3.2	78.3 ± 39.2	0.0 ± 0.0	3.0 ± 1.5	81.3 ± 39.2	120 ± 119 (103)
Winter (DJF)	212 ± 40 (163)	8.0 ± 4.0	31.4 ± 15.7	8.2 ± 4.1	-25.6 ± 12.8	14.0 ± 20.7	201 ± 45 (190)
West							
	Air-sea TOI flux	Non-steady state	Physical supply				Gross oxygen production (GOP)
			Vertical supply	Upwelling	Horizontal convergence	Sum	
Spring (MAM)	195 ± 62 (85)	9.4 ± 4.7	3.6 ± 1.8	1.5 ± 0.8	1.1 ± 0.5	6.2 ± 2.0	197 ± 62 (79)
Summer (JJA)	117 ± 21 (54)	-0.4 ± 0.2	22.4 ± 11.2	2.1 ± 1.1	-2.1 ± 1.0	22.5 ± 11.3	93 ± 24 (38)
Fall (SON)	183 ± 30 (104)	-5.1 ± 2.5	64.0 ± 32.0	-1.5 ± 0.7	-0.2 ± 0.1	62.2 ± 32.0	118 ± 44 (71)
Winter (DJF)	191 ± 32 (126)	1.0 ± 0.5	38.9 ± 19.4	10.2 ± 5.1	-5.5 ± 2.8	43.6 ± 20.3	137 ± 38 (93)
East							
	Air-sea TOI flux	Non-steady state	Physical supply				Gross oxygen production (GOP)
			Vertical supply	Upwelling	Horizontal convergence	Sum	
Spring (MAM)	167 ± 23 (64)	9.4 ± 4.7	8.8 ± 4.4	-1.8 ± 0.9	1.2 ± 0.6	8.2 ± 4.5	167 ± 23 (58)
Summer (JJA)	91 ± 15 (42)	-0.8 ± 0.4	32.3 ± 16.2	-2.3 ± 1.1	2.3 ± 1.1	32.3 ± 16.2	58 ± 22 (26)
Fall (SON)	156 ± 24 (99)	-4.9 ± 2.5	63.3 ± 31.6	-7.8 ± 3.9	2.5 ± 1.3	58.0 ± 31.9	92 ± 40 (57)
Winter (DJF)	134 ± 18 (83)	3.4 ± 1.7	33.6 ± 16.8	2.2 ± 1.1	-2.5 ± 1.2	33.4 ± 16.9	102 ± 24 (57)

[a] All GOP budget terms in units of mmol O_2 m^{-2} d^{-1}. Uncertainty, incorporating methodological error and undersampling bias, is given for each budget term (details in text, section 2.5). The standard deviations of all discrete points included in the calculated means for air-sea TOI flux and of GOP, representing spatial and temporal variability in the region, are given in parentheses. All terms are calculated following equation (2), which can be represented as: GOP = Air-sea TOI flux + Non-steady state – Physical supply of TOI.

Table S3: Seasonal means for each region for all terms in the net community production (NCP) mixed layer budget[a]

Kuroshio									
	Air-sea O_2/Ar flux	Non-steady state	Physical supply						Net community production (NCP)
			Entrainment	Vertical diffusion	Upwelling	Ekman convergence	Geostrophic convergence	Sum	
Spring (MAM)	8.9 ± 2.0 (27.1)	3.6 ± 1.8	-0.5 ± 0.2	-11.7 ± 5.8	-0.3 ± 0.2	0.2 ± 0.1	-2.3 ± 1.1	-14.5 ± 6.0	27.2 ± 6.5 (29.5)
Summer (JJA)	13.3 ± 2.2 (12.4)	0.5 ± 0.2	0.0 ± 0.0	-0.2 ± 0.1	0.0 ± 0.0	-0.1 ± 0.1	-1.9 ± 1.0	-2.2 ± 1.0	16.2 ± 2.4 (17.6)
Fall (SON)	20.5 ± 11.4 (14.9)	-2.6 ± 1.3	-1.3 ± 0.6	-1.4 ± 0.7	-0.1 ± 0.0	-0.1 ± 0.0	1.1 ± 0.5	-1.7 ± 1.1	20.0 ± 11.6 (16.5)
Winter (DJF)	-53.0 ± 9.8 (49.2)	-0.8 ± 0.4	-20.4 ± 10.2	-25.1 ± 12.6	-2.8 ± 1.4	0.4 ± 0.2	-3.9 ± 1.9	-51.8 ± 16.4	0.0 ± 19.1 (85.4)
West									
	Air-sea O_2/Ar flux	Non-steady state	Physical supply						Net community production (NCP)
			Entrainment	Vertical diffusion	Upwelling	Ekman convergence	Geostrophic convergence	Sum	
Spring (MAM)	3.8 ± 1.7 (10.6)	2.6 ± 1.3	-5.6 ± 2.8	-0.8 ± 0.4	-3.9 ± 2.0	0.0 ± 0.0	-3.5 ± 1.7	-13.8 ± 3.9	20.9 ± 4.4 (24.0)
Summer (JJA)	13.5 ± 2.5 (15.3)	0.4 ± 0.2	0.0 ± 0.0	0.0 ± 0.0	-0.3 ± 0.1	0.1 ± 0.1	-1.2 ± 0.6	-1.3 ± 0.6	14.9 ± 2.6 (17.2)
Fall (SON)	16.0 ± 2.7 (12.6)	-1.6 ± 0.8	0.4 ± 0.2	0.0 ± 0.0	-0.1 ± 0.1	0.4 ± 0.2	-1.2 ± 0.6	-0.6 ± 0.7	15.2 ± 2.8 (11.2)
Winter (DJF)	-17.7 ± 3.1 (29.7)	-1.7 ± 0.8	-10.2 ± 5.1	-1.8 ± 0.9	-4.2 ± 2.1	-0.6 ± 0.3	-3.7 ± 1.8	-20.5 ± 5.9	0.0 ± 6.7 (33.6)
East									
	Air-sea O_2/Ar flux	Non-steady state	Physical supply						Net community production (NCP)
			Entrainment	Vertical diffusion	Upwelling	Ekman convergence	Geostrophic convergence	Sum	
Spring (MAM)	7.4 ± 1.2 (16.4)	0.8 ± 0.4	-3.8 ± 1.9	-0.6 ± 0.3	-0.2 ± 0.1	0.2 ± 0.1	-0.2 ± 0.1	-4.6 ± 1.9	12.8 ± 2.3 (18.7)
Summer (JJA)	5.0 ± 0.9 (7.7)	0.3 ± 0.1	0.1 ± 0.1	0.2 ± 0.1	0.0 ± 0.0	-0.1 ± 0.0	-0.3 ± 0.1	0.1 ± 0.2	5.3 ± 0.9 (8.1)
Fall (SON)	19.4 ± 3.0 (9.6)	-0.9 ± 0.4	0.4 ± 0.2	0.0 ± 0.0	0.0 ± 0.0	-0.1 ± 0.0	-0.4 ± 0.2	0.0 ± 0.3	18.7 ± 3.0 (11.4)
Winter (DJF)	2.0 ± 0.4 (16.2)	-1.4 ± 0.7	-2.7 ± 1.4	-0.6 ± 0.3	-0.5 ± 0.3	0.0 ± 0.0	0.9 ± 0.5	-3.0 ± 1.5	3.5 ± 1.7 (17.7)

[a] All NCP budget terms in units of mmol O_2 m^{-2} d^{-1}. Uncertainty, incorporating methodological error and undersampling bias, is given for each budget term (details in text, section 2.5). The standard deviations of all discrete points included in the calculated means for air-sea O_2/Ar flux and of NCP, representing spatial and temporal variability in the region, are given in parentheses. All terms are calculated following equation (4), which can be represented as: NCP = Air-sea O_2/Ar flux + Non-steady state – Physical supply of O_2/Ar.

Table S4: Annual means for each region for all terms in the annual GOP and NCP budgets[a]

		Kuroshio	West	East
AGOP budget				
Air-sea TOI flux (euphotic zone AGOP)		74.3 ± 20.1	62.6 ± 11.8	50.1 ± 7.2
Vertical supply		16.3 ± 17.9	14.3 ± 11.8	12.6 ± 14.4
Upwelling		0.5 ± 1.5	1.1 ± 1.9	-0.9 ± 1.6
Horizontal convergence		-2.9 ± 4.9	-0.6 ± 1.1	0.3 ± 0.8
Mixed layer annual GOP		60.0 ± 21.7	49.3 ± 13.2	37.5 ± 9.5
ANCP budget				
Air-sea O_2/Ar flux		-0.95 ± 1.19	1.42 ± 0.32	3.09 ± 0.48
Mixed layer horizontal convergence	Ekman	0.03 ± 0.08	0.00 ± 0.13	0.01 ± 0.04
	Geostrophic	-0.64 ± 0.91	-0.87 ± 0.97	0.00 ± 0.19
Sub-mixed layer horizontal convergence	Ekman	-0.01 ± 0.00	0.00 ± 0.00	-0.04 ± 0.02
	Geostrophic	-0.06 ± 0.03	0.52 ± 0.26	-0.07 ± 0.03
Upwelling across base of winter mixed layer		-0.97 ± 0.49	-0.90 ± 0.45	-0.07 ± 0.03
ANCP to winter ventilation depth		0.70 ± 1.02	2.68 ± 0.76	3.26 ± 0.48

[a] All budget terms in units of mol O_2 m^{-2} yr^{-1}. Uncertainty, incorporating methodological error and undersampling bias, is given for each budget term (details in text, section 2.5). Euphotic zone AGOP is equivalent to the annual air-sea TOI flux. Mixed layer annual GOP (calculated as the annual integral of the seasonal GOP budget following equation 2) = Annual air-sea TOI flux – Vertical supply – Upwelling – Horizontal convergence. ANCP to the winter ventilation depth (calculated following equation 8) = Annual air-sea O_2/Ar flux – Mixed layer horizontal convergence – Sub-mixed layer horizontal convergence – Upwelling across the base of the winter mixed layer.

References

Craig, H., and T. Hayward (1987), Oxygen supersaturation in the ocean: Biological versus physical contributions, *Science*, *235*, 199–202.

Howard, E., S. Emerson, S. Bushinsky, and C. Stump (2010), The role of net community production in air-sea carbon fluxes at the North Pacific subarctic-subtropical boundary region, *Limnol. Oceanogr.*, *55*(6), 2585–2596, doi:10.4319/lo.2010.55.6.2585.

Lockwood, D. E. (2013), Impact of the marine biological pump on atmospheric CO_2 uptake in the North Pacific: a study based on basin-wide underway measurements of oxygen/argon gas ratios and pCO_2, Ph.D. thesis, University of Washington, Seattle, Washington.